Inorganic Chemistry

Article

pubs.acs.org/IC

Time Resolved Infrared Spectroscopy: Kinetic Studies of Weakly Binding Ligands in an Iron–Iron Hydrogenase Model Compound

Sohail Muhammad,[†] Salvador Moncho,[†] Edward N. Brothers,[†] Marcetta Y. Darensbourg,[‡] Donald J. Darensbourg,*[,‡] and Ashfaq A. Bengali*[,†]

[†]Department of Chemistry, Texas A&M University at Qatar, Doha, Qatar

[‡]Department of Chemistry, Texas A&M University, College Station, Texas 77843, United States

Supporting Information

ABSTRACT: Solution photochemistry of (μ-pdt)[Fe(CO)$_3$]$_2$ (pdt = μ_2-S(CH$_2$)$_3$S), a precursor model of the 2-Fe subsite of the H-cluster of the hydrogenase enzyme, has been studied using time-resolved infrared spectroscopy. Following the loss of CO, solvation of the Fe center by the weakly binding ligands cyclohexene, 3-hexyne, THF, and 2,3-dihydrofuran (DHF) occurred. Subsequent ligand substitution of these weakly bound ligands by pyridine or cyclooctene to afford a more stable complex was found to take place via a dissociative mechanism on a seconds time scale with activation parameters consistent with such a pathway. That is, the $\Delta S^{\ddagger}$ values were positive and the $\Delta H^{\ddagger}$ parameters closely agreed with bond dissociation enthalpies (BDEs) obtained from DFT calculations. For example, for cyclohexene replacement by pyridine, experimental $\Delta H^{\ddagger}$ and $\Delta S^{\ddagger}$ values were determined to be 19.7 ± 0.6 kcal/mol (versus a theoretical prediction of 19.8 kcal/mol) and 15 ± 2 eu, respectively. The ambidentate ligand 2,3-DHF was shown to initially bind to the iron center via its oxygen atom followed by an intramolecular rearrangement to the more stable η^2-olefin bound species. DFT calculations revealed a transition state structure with the iron atom almost equidistant from the oxygen and one edge of the olefinic bond. The computed $\Delta H^{\ddagger}$ of 10.7 kcal/mol for this isomerization process was found to be in excellent agreement with the experimental value of 11.2 ± 0.3 kcal/mol.

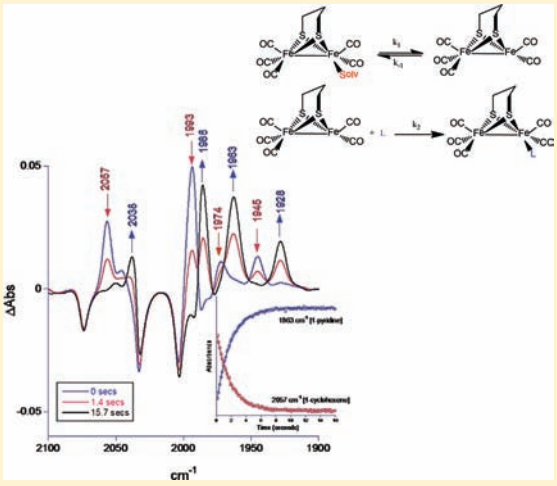

INTRODUCTION

The considerable chemical literature developed in the past decade relevant to biomimetics of the diiron hydrogenase, [FeFe]-H$_2$ase, enzyme active site (eas) has been inspired by the challenge to produce a catalyst for hydrogen production or uptake derived from the earth abundant iron metal rather than platinum which is currently used in fuel cells.[1] Synthetic progress in this area has been facilitated by the availability of a singular synthon, (μ-S$_2$)[Fe(CO)$_3$]$_2$, and a derivative that reproduces several features of the eas, (μ-pdt)[Fe(CO)$_3$]$_2$ [(μ-pdt) = (μ_2-SCH$_2$CH$_2$CH$_2$S)], designated in this manuscript as **1**-CO. Stable with various S to S linkers, and capable of other modifications including CO/L ligand exchange, synthetic progress has led to diiron complexes that serve as solution electrocatalysts for proton reduction to H$_2$; with suitable modification of the S to S linker, the overpotential can be optimized to approaching the efficiency of platinum.[2] Further analysis of the features that control the unique geometry of the diiron unit in the eas has led to synthetic analogues in a conformation heretofore unknown in organometallic chemistry, and to rarely observed mixed-valent Fe^{I}Fe^{II} complexes that are stable in the rotated conformation of edge-bridged square pyramids as seen in the eas.[3−5]

Beyond the features of **1**-CO that are similar to the [FeFe]-H$_2$ase enzyme active site, the (μ-pdt)[Fe(CO)$_3$]$_2$ complex has properties of fundamental interest, especially CO photolability that clearly leads to coordinative unsaturation and subsequent recapture of CO or to binding of both weak and strong donor entities.[6−11] Recent work in this area with ultrafast time-resolved IR spectroscopy has shown photoinduced isomerization of the tricarbonyl intermediate produced when (μ-pdt)[Fe(CO)$_2$PMe$_3$]$_2$ undergoes UV photolysis, accessing in this process the thermodynamically less stable apical/basal isomer.[7] Solvent dependencies of rates indicate a role for polar solvent (MeOH, CH$_3$CN) coordination to the intermediate that competes with CO recombination.[7]

Herein we report probes of the coordinatively unsaturated (μ-pdt)[Fe$_2$(CO)$_5$] (**1**) fragment in the presence of Solv = cyclohexene, 3-hexyne, THF, and 2,3-dihydrofuran (DHF) and L = *cis*-cyclooctene and pyridine yielding spectroscopically observable **1**-Solv and **1**-L adducts. The mechanism and energetics of solvent displacement from the **1**-Solv complexes were studied with a view toward obtaining fundamental

Received: April 16, 2012
Published: June 8, 2012

   dx.doi.org/10.1021/ic300785z | *Inorg. Chem.* 2012, 51, 7362−7369

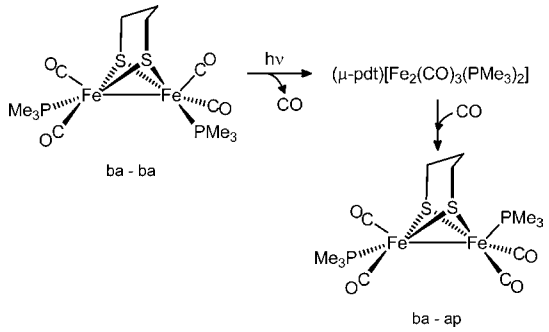

information about the reactivity of these species. Since displacement of Solv from these complexes was found to proceed through a dissociative pathway, the **1**-Solv bond enthalpies were estimated. The **1**-DHF derivative shows that DHF may act as an ambidentate ligand, binding initially as the kinetic isomer through the oxygen, and subsequently isomerize to the η^2-olefin-bound DHF, presumed to be the thermodynamically stable isomer.

EXPERIMENTAL AND THEORETICAL METHODS

A Bruker Vertex 80 FTIR was used in rapid scan mode for all the kinetic studies. Spectra were taken at 4 and 8 cm^{-1} resolution for the characterization of the CO stretching band positions and the kinetic studies, respectively. Solution photolysis was conducted using 355 nm light from a Continuum Surelite I-10 laser. A temperature controlled 0.75 mm path length IR cell with CaF_2 windows (Harrick Scientific) was used for sample photolysis at temperatures ≥288 K. A variable temperature cell (Graesby-Specac) equipped with a 0.5 mm path length flow cell with CaF_2 windows was used for the low temperature experiments. To avoid complications due to multiple photolysis effects, all spectra were obtained using a single shot of the UV pump laser.

Typically, the photolysis solution contained 1 mg/mL of **1**-CO dissolved in cyclohexane with the appropriate amount of Solv or L added. For the kinetic experiments involving the displacement of THF and cyclohexene, from **1**-THF and **1**-(η^2-cyclohexene), **1**-CO was dissolved in these solvents and increasing amounts of *cis*-cyclooctene and pyridine as the displacing ligand were added, respectively. For the substitution of 3-hexyne and η^2-DHF, **1**-CO was dissolved in cyclohexane containing 3-hexyne or DHF, and pyridine was added as the incoming ligand. In most cases, the kinetic experiments were conducted over a 10-fold range of incoming ligand concentrations and a 20−30 K temperature range. Observed rate constants (k_{obs}) were obtained by first-order fits to the temporal profile of either reactant decay or product growth. The stated errors in the rate constants and activation parameters were obtained from least-squares fit to the data as reported by the data analysis program Kaleidagraph.

The **1**-CO complex was synthesized according to literature procedure.[12] All reagents (Aldrich) were of >99% purity with the exception of *cis*-cyclooctene which was of >95% purity. Cyclohexane, THF, and pyridine were anhydrous grade.

All calculations were performed in the development version of the Gaussian suite of programs using density functional theory (DFT).[13] Energies, frequencies, and stationary point geometries were obtained using the ωB97XD functional[14] and the def2-TZVPP basis set.[15] While some elements in def2-TZVPP utilize pseudopotentials, the elements considered in this study did not. The computed geometries were confirmed to be ground state structures or transition states according to their number of imaginary frequencies. If not stated otherwise, the energies reported in the text are enthalpies computed at 298.15 K and 1 atm, and are expressed in kcal/mol.

RESULTS AND DISCUSSION

Previous studies have demonstrated that UV photolysis of **1**-CO in solution phase results in the dissociation of a CO ligand

Scheme 1

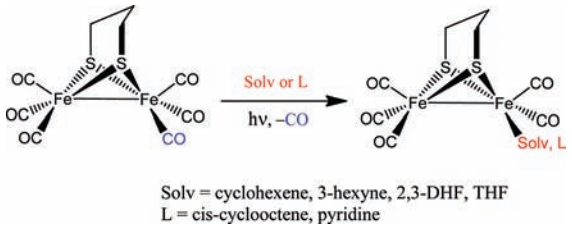

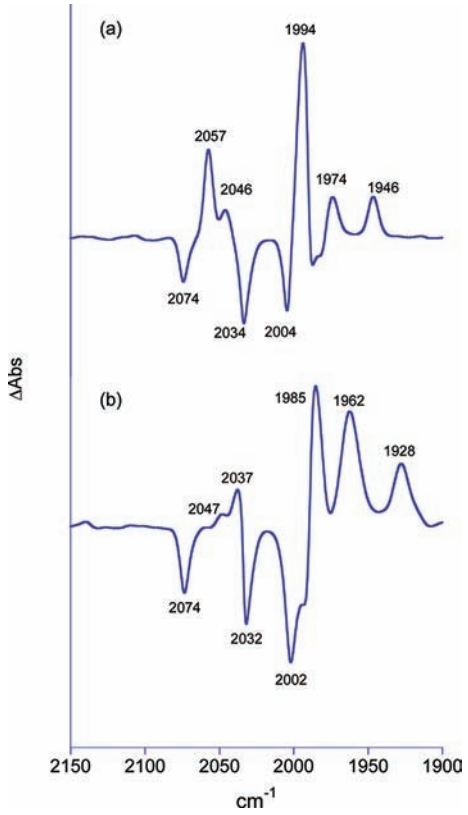

Figure 1. Difference FTIR spectra obtained upon photolysis of a cyclohexane solution of **1**-CO in the presence of (a) cyclohexene and (b) pyridine at 293 K.

Table 1. CO Band Positions for Several Complexes

complex	ν_{CO} (cm^{-1}) (cyclohexane)
1-(η^2-cyclooctene)	1951, 1974, 1998, 2047, 2057
1-(η^2-cyclohexene)	1946, 1974, 1994, 2046, 2057
1-(η^2-3-hexyne)	1946, 1972, 1994, 2045, 2056
1-(η^2-DHF)	1942, 1969, 1993, 2045, 2054
1-(η^1-O−DHF)	1926, 1960, 1984, 2041
1-THF	1923, 1961, 1983, 2040, 2051
1-pyridine	1928, 1962, 1985, 2037, 2047

followed by ultrafast coordination of solvent to yield **1**-Solv.[10] Our results are consistent with these and other longer time scale experiments (Scheme 1).[8,9] Spectral changes following photolysis of a cyclohexane solution of **1**-CO in Solv = cyclohexene or L = pyridine are shown in Figure 1 while those for Solv = 3-hexyne, η^2-DHF, THF and L = *cis*-cyclooctene are presented in the Supporting Information. The spectral changes are consistent with the formation of the respective **1**-Solv and **1**-L complexes. For each complex five CO stretching absorbances are observed consistent with the reduced

dx.doi.org/10.1021/ic300785z | Inorg. Chem. 2012, 51, 7362−7369

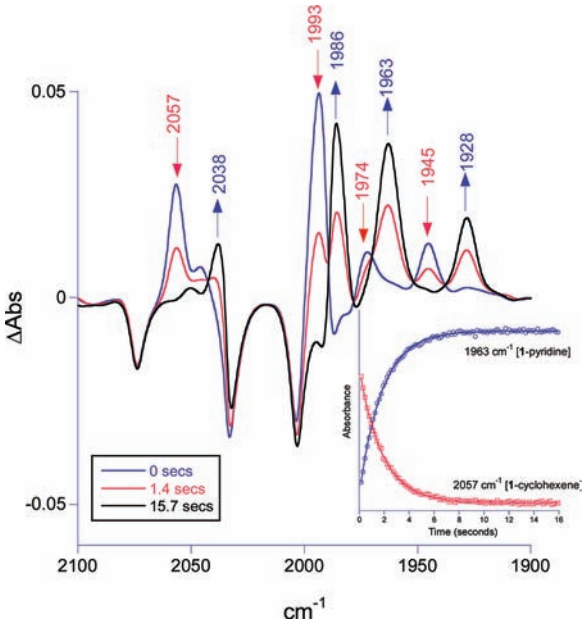

Figure 2. Spectral changes upon photolysis of a cyclohexene solution of **1**-CO in the presence of pyridine. The peaks marked ↑ are due to the growth of the **1**-pyridine complex while those marked ↓ are due to the decay of the **1**-(η^2-cyclohexene) reactant.

symmetry of the **1**-Solv and **1**-L species.[8,9] The absence of additional CO bands suggests the formation of only one isomer which is assumed to be the thermodynamically favored basal structure.[7]

The ν_{CO} positions for all the complexes studied are listed in Table 1. The spectral characteristics in the CO stretching region are similar for all **1**-Solv species with almost identical peak locations for Solv = cyclooctene, cyclohexene, η^2 coordinated DHF, and 3-hexyne. Consistent with the stronger σ donor ability of THF, η^1-DHF, and pyridine, CO bands for these complexes are red-shifted relative to the other molecules.

a. Kinetic Studies. When photolysis of **1**-CO is conducted in the presence of both Solv and L, spectral changes are observed that are consistent with the displacement of the solvent from the initially formed **1**-Solv adduct to yield the respective **1**-L complex. For example, as shown in Figure 2, photolysis of a cyclohexene solution of **1**-CO in the presence of pyridine results in the formation of the **1**-(η^2-cyclohexene) complex which then undergoes a first-order conversion to the thermodynamically stable **1**-pyridine complex[16] which grows in at the same rate. Similarly, photolysis of **1**-CO in THF in the presence of cyclooctene results in the displacement of THF from the solvate to form **1**-(η^2-cyclooctene). Complete kinetics analyses for the reactions shown in Scheme 2 were conducted.

Since reactions a and b were faster than c and d and the reaction rates were inversely proportional to the concentration of the departing ligand, they were conducted in pure THF and cyclohexene solvent. For the remaining reactions, cyclohexane was used as a diluent and the concentration of DHF and 3-hexyne was held constant at 3.3 and 2.2 M, respectively, as pyridine was added.

Scheme 2

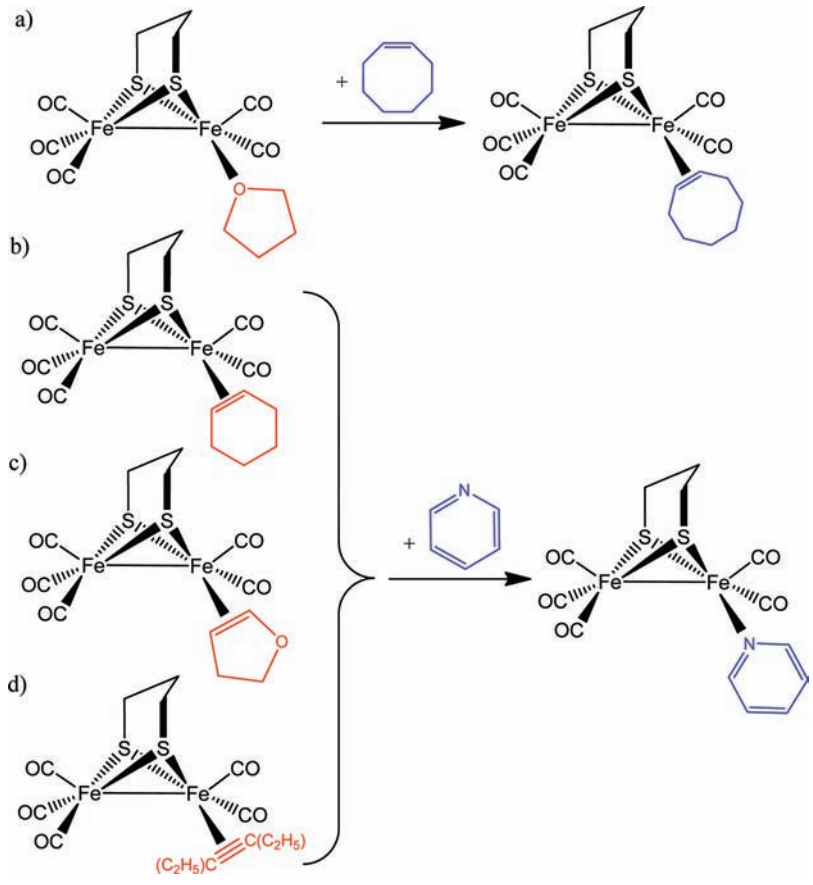

dx.doi.org/10.1021/ic300785z | Inorg. Chem. 2012, 51, 7362−7369

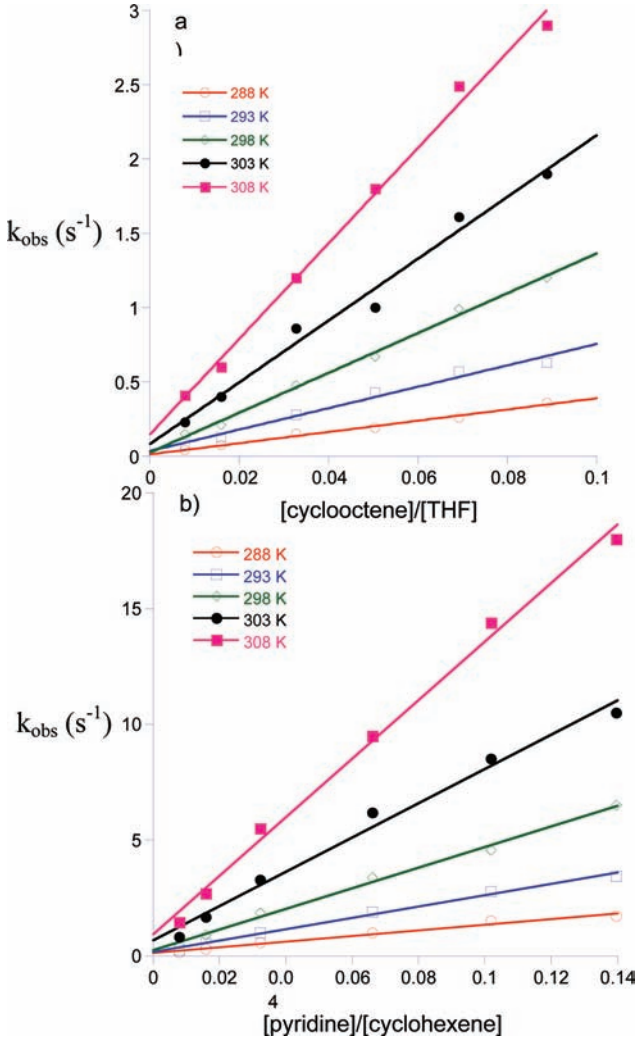

Figure 3. Plots of k_{obs} vs [L]/[Solv] for (a) L = cyclooctene, Solv = THF, and (b) L = pyridine, Solv = cyclohexene.

Scheme 3

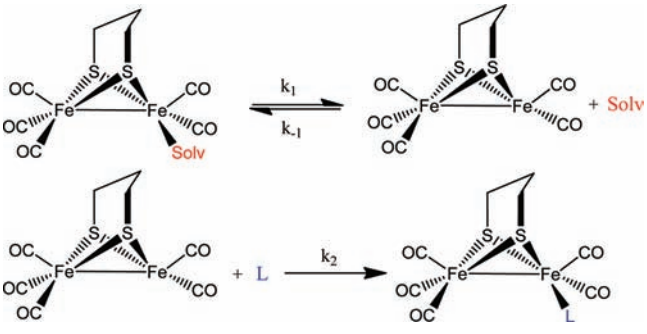

As shown in Figure 3, k_{obs} exhibits a linear dependence on the incoming ligand concentration for both reactions a and b. Such dependence is consistent with associative, dissociative, or interchange mechanisms of solvent displacement.[17] However, as noted above, k_{obs} is inversely proportional to the concentration of the solvent. For example, for reaction a at 298 K with cyclohexane added as the diluent and [cyclooctene] = 0.19 M, k_{obs} increases from 0.32 to 0.67 s^{-1} as [THF] is decreased from 2.1 to 0.91 M. This inverse dependence of k_{obs} is consistent with a mechanism that involves reversible

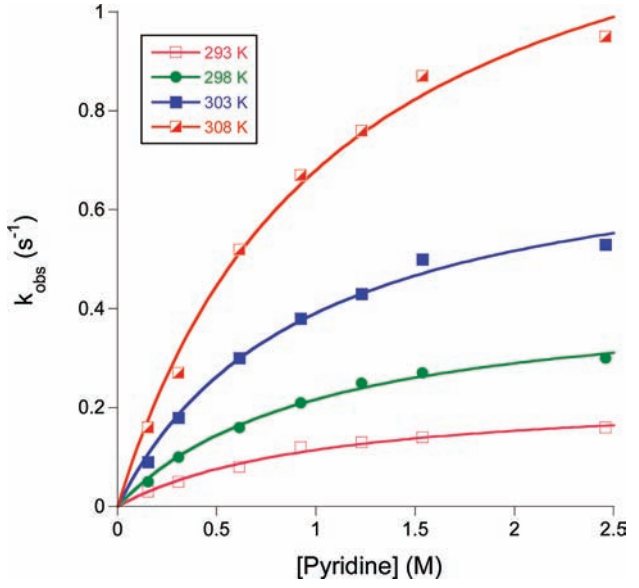

Figure 4. Plot of k_{obs} vs [pyridine] for the reaction: **1**-(η^2-3-hexyne) + pyridine → **1**-pyridine + 3-hexyne.

dissociation of the solvent molecule prior to formation of the product **1**-L complex (Scheme 3).

Application of the steady state assumption to intermediate **1** yields the k_{obs} dependence shown in eq 1.

$$k_{obs} = \frac{k_1 k_2[L]}{k_{-1}[Solv] + k_2[L]} \quad (1)$$

If $k_{-1}[Solv] > k_2[L]$, which is likely the case here since the reactions were conducted using pure THF and cyclohexene as solvent (i.e., [Solv] > [L]), k_{obs} will exhibit a linear dependence on [L]/[Solv] as observed. The slope of the k_{obs} versus [L]/[Solv] plots are therefore expected to yield the collection of rate constants k_1k_2/k_{-1}. Further evidence for a dissociative substitution mechanism is evident from the kinetics of reactions c and d for Solv = DHF and 3-hexyne, respectively. In these reactions, [3-hexyne] and [DHF] were held constant as [pyridine] was varied, and it was possible to achieve conditions where [Solv] ≈ [L]. Consistent with eq 1, and as shown in Figure 4, k_{obs} exhibits saturation behavior at high [pyridine] and a fit of the data to eq 1 yields k_1 and the selectivity ratio k_2/k_{-1}. The relevant rate constants for all the reactions studied are presented in Table 2.

Since the substitution reactions appear to follow a dissociative mechanism in all cases, the temperature dependence of the rate constants can provide an estimate for the binding enthalpies of THF, cyclohexene, η^2-DHF, and 3-hexyne to **1**. As mentioned earlier, for Solv = THF and cyclohexene, the slope of the k_{obs} versus [L]/[Solv] plot yields the collection of rate constants k_1k_2/k_{-1}. Since 16 e^- complexes often react with substrates without a significant activation barrier,[18] it is reasonable to conclude that $\Delta H^{\ddagger}_2 \approx \Delta H^{\ddagger}_{-1} \approx 0$. Therefore, from the temperature dependence of k_1k_2/k_{-1}, an estimate for $\Delta H^{\ddagger}_1$ may be obtained which is expected to approximate the **1**-THF and **1**-(η^2-cyclohexene) bond dissociation enthalpy (BDE).

Since k_1 is extracted directly from the limiting value of k_{obs} in the case of Solv =3-hexyne and DHF no assumptions are required to obtain $\Delta H^{\ddagger}_1$ in this case. Eyring plots for Solv = THF, cyclohexene, DHF, and 3-hexyne are shown in Figure 5.

dx.doi.org/10.1021/ic300785z | Inorg. Chem. 2012, 51, 7362−7369

Table 2. Rate Constants and Activation Parameters Obtained from the k_{obs} Dependence on Incoming Ligand Concentration and Temperature for the 1-Solv + L → 1-L + Solv Reactions

			3-hexyne[c]		η^2-DHF[d]	
T (K)	THF[a] k_1k_2/k_{-1} (s^{-1})	cyclohexene[b] k_1k_2/k_{-1} (s^{-1})	k_1 (s^{-1})	k_2/k_{-1}	k_1 (s^{-1})	k_2/k_{-1}
288	3.8 ± 0.2	12.2 ± 0.9			0.40 ± 0.06	2.1 ± 0.5
293	7.2 ± 0.5	24.5 ± 1.1	0.23 ± 0.02	2.2 ± 0.4	0.62 ± 0.10	3.0 ± 0.9
298	13.4 ± 0.5	44.5 ± 1.6	0.44 ± 0.02	2.2 ± 0.3	1.34 ± 0.20	2.3 ± 0.6
303	20.8 ± 1.3	74.0 ± 4.4	0.76 ± 0.05	2.3 ± 0.3	2.46 ± 0.43	2.1 ± 0.6
308	32.1 ± 1.2	126.5 ± 4.9	1.42 ± 0.09	2.0 ± 0.3		

[a] $\Delta H^{\ddagger}$ = 18.2 ± 0.9 kcal/mol, $\Delta S^{\ddagger}$ = 8 ± 3 eu. [b] $\Delta H^{\ddagger}$ = 19.7 ± 0.6 kcal/mol, $\Delta S^{\ddagger}$ = 15 ± 2 eu. [c] $\Delta H_1^{\ddagger}$ = 20.9 ± 0.4 kcal/mol, $\Delta S^{\ddagger}$ = 10 ± 2 eu. [d] $\Delta H_1^{\ddagger}$ = 20.9 ± 1.6 kcal/mol, $\Delta S^{\ddagger}$ = 12 ± 5 eu.

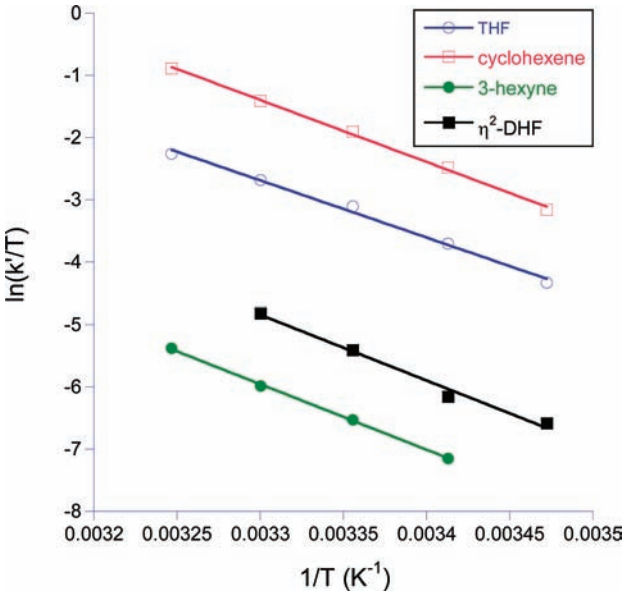

Figure 5. Eyring plots for the reaction **1**-Solv → **1** + Solv. For Solv = cyclohexene and THF, $k' = k_1k_2/k_{-1}$ while for Solv = 3-hexyne, η^2-DHF $k' = k_1$.

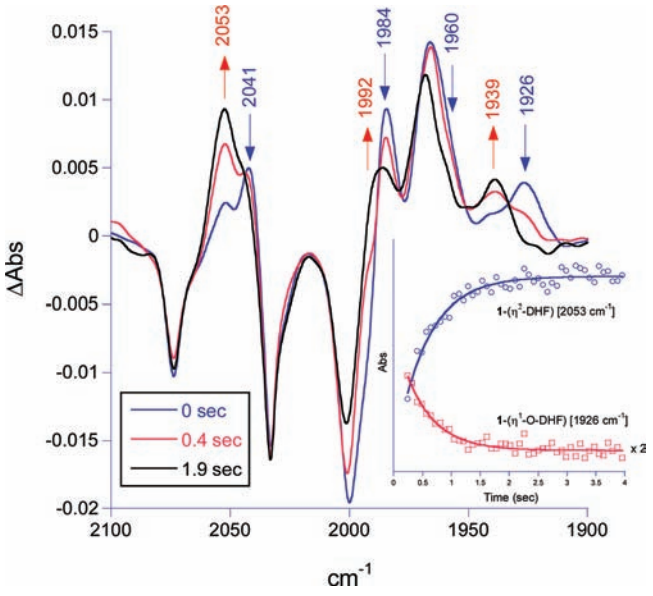

Figure 6. Spectral changes observed upon photolysis of a cyclohexane solution of **1**-CO in the presence of 6.6 M DHF at 223 K. By comparison with the CO band positions of the **1**-(η^2-DHF) and **1**-THF complexes, the peaks marked with ↓ are due to the **1**-(η^1-O–DHF) isomer which converts to the thermodynamically favored **1**-(η^2-DHF) complex whose peaks are marked with ↑.

Table 3. 1-Solv Binding Enthalpies for Several Complexes

complex	BDE(calcd) kcal/mol	$\Delta H^{\ddagger}$ (exptl) kcal/mol
1-CO	37.4	
1-(η^2-toluene)	12.7	
1-(η^2-cyclohexene)	19.8	19.7 ± 0.6
1-(η^2-3-hexyne)	21.3	20.9 ± 0.4
1-(η^2-DHF)	20.5	20.9 ± 1.6
1-(η^1-O–DHF)	18.9	
1-THF	22.7	18.2 ± 0.9

The positive $\Delta S^{\ddagger}$ values for all the reactions are consistent with the dissociative mechanistic assignment. As shown in Table 2, of the four solvents studied, THF has the weakest while cyclohexene, 3-hexyne, and η^2-DHF have similar binding strengths to **1**. Other metal complexes also exhibit a similar trend. For example, the [Mn]–THF bond is weaker than the [Mn]–(η^2-alkene) interaction ([M] = $CpMn(CO)_2$) although the ≈10 kcal/mol difference in binding enthalpy is greater than the ≈2 kcal/mol difference in the bond strengths in the present systems.[19,20] To lend support for the experimental findings, DFT calculations were performed on the relevant systems, and consistent with dissociative displacement of the solvent molecules from **1**-Solv, the calculated BDEs are in good agreement with the experimental activation enthalpies (Table 3).

b. Linkage Isomerism. It is evident that photolysis of **1**-CO in THF or cycloalkene solvent leads to **1**-THF and **1**-(η^2-cycloalkene), respectively. We therefore considered the possibility of linkage isomer formation if **1**-CO were to be photolyzed in the presence of a solvent that had both alkene and oxygen binding sites. When a cyclohexane solution of **1**-CO containing 6.6 M of the ambidentate DHF solvent was photolyzed at room temperature, only the η^2 complex was observed (Supporting Information). This complex was identified as the η^2 isomer by comparison of the observed CO peak locations with those of **1**-(η^2-cyclooctene) and **1**-(η^2-cyclohexene). Interestingly, as shown in Figure 6, when the photolysis was carried out at 223 K,[21] additional peaks were observed which when compared with the **1**-THF species were consistent with the transient formation of the **1**-(η^1-O–DHF) complex. The oxo bound isomer converts to the η^2 isomer within 2 s at this temperature (Scheme 4).

The isomerization reaction was studied over a 20 K range, and the resulting Eyring plot is shown in Figure 7. The $\Delta H^{\ddagger}$ value of 11.2 ± 0.3 kcal/mol is considerably lower than the **1**-

dx.doi.org/10.1021/ic300785z | Inorg. Chem. 2012, 51, 7362–7369

Scheme 4

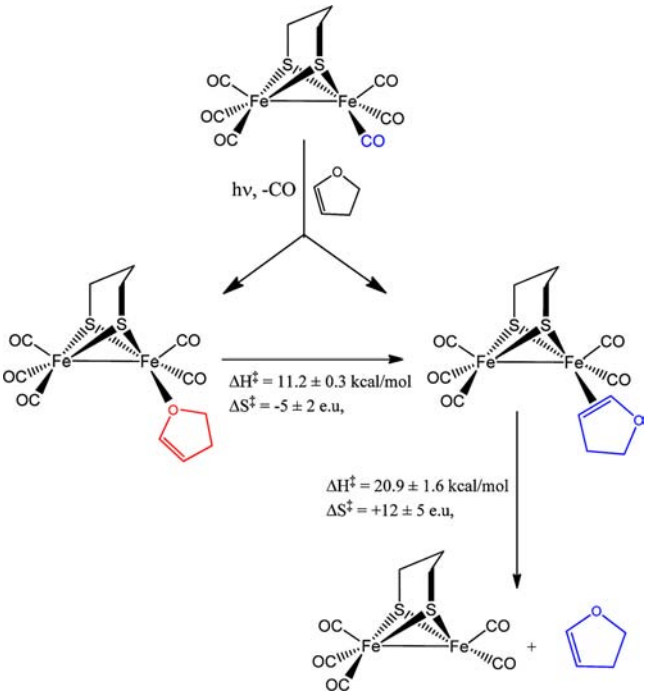

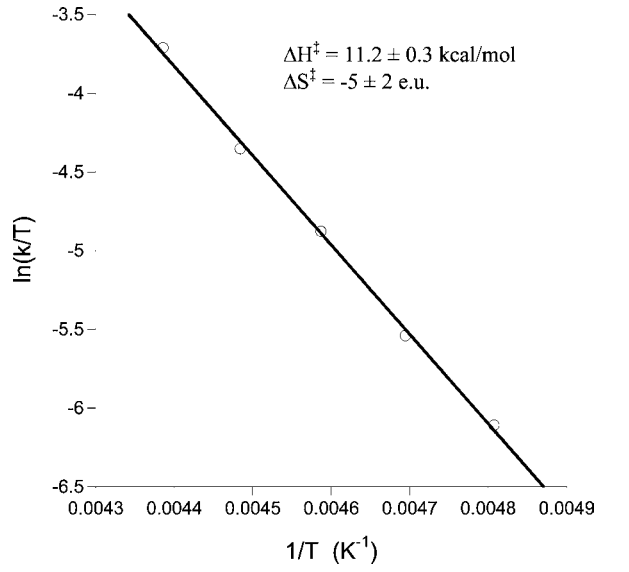

Figure 7. Eyring plot for the isomerization reaction: **1**-(η^1-O−DHF) → **1**-(η^2-DHF).

THF BDE estimated at 18.2 kcal/mol. Due to the delocalization of the oxygen lone pairs in DHF, the **1**-(η^1-O−DHF) BDE is expected to be slightly lower than that of **1**-THF consistent with theoretical estimates (Table 3). However, the large difference in the isomerization activation enthalpy and **1**-THF binding enthalpy suggests that the transition state for the isomerization reaction does not involve significant disruption of the **1**-(η^1-O−DHF) bond, or if it does, then concomitant interaction with the olefinic carbons lowers the activation enthalpy. Similar to the previously observed $CpMn(CO)_2(\eta^1$-O−DHF) → $CpMn(CO)_2(\eta^2$-DHF) conversion,[22] the isomerization likely proceeds through a concerted, intramolecular pathway which involves the Fe metal migrating from the oxygen to the C═C binding site.

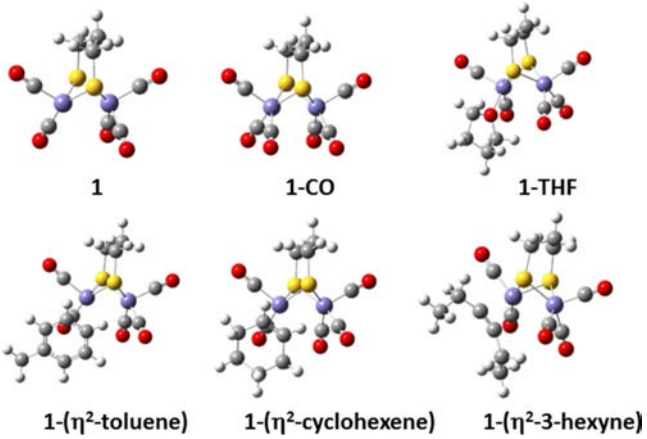

Figure 8. Calculated structures for several **1**-Solv complexes including the parent **1**-CO.

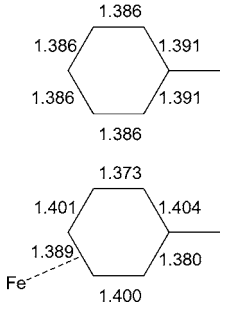

Figure 9. Calculated C−C bond lengths in complexed and uncomplexed toluene.

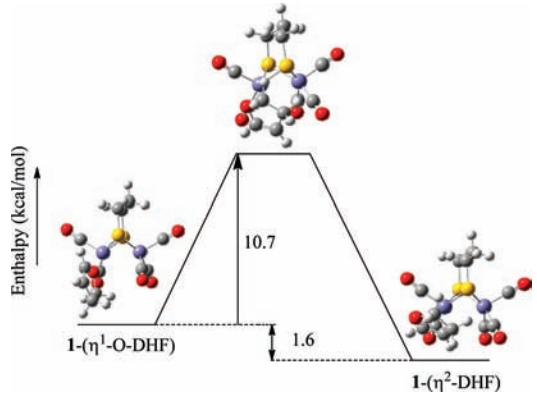

Figure 10. Calculated enthalpic profile for the isomerization reaction **1**-(η^1-O−DHF) → **1**-(η^2-DHF).

c. Theoretical Modeling. To provide support for the experimental findings, DFT calculations were performed on the relevant systems. The calculated structures for **1**, **1**-CO, and several **1**-Solv complexes are displayed in Figure 8.

Binding of either cyclohexene, 3-hexyne, or η^2-DHF to **1** results in only a 2−3% lengthening of the C═C and C≡C bonds relative to the free molecules suggestive of only a modest Fe → π backbonding interaction. The **1**-(η^2-toluene) complex was also modeled since it has been observed previously.[8] Consistent with the aromatic stabilization of toluene, the **1**-(η^2-toluene) binding interaction is calculated to be significantly weaker relative to olefin coordination. Interestingly, as shown in Figure 9, η^2 binding of toluene results in localization of the

dx.doi.org/10.1021/ic300785z | Inorg. Chem. 2012, 51, 7362−7369

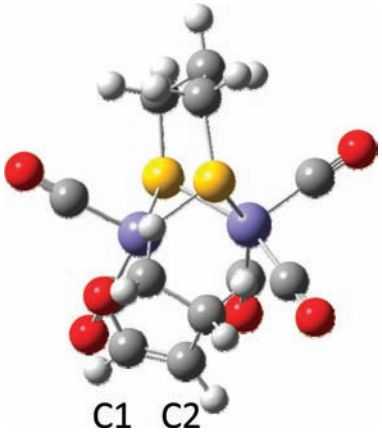

Figure 11. Calculated transition state structure for the isomerization reaction **1**-(η^1-O–DHF) → **1**-(η^2-DHF).

electron density in the aromatic ring system such that the C—C bond lengths are no longer the same as in the uncomplexed molecule.

Importantly, the calculated BDEs for all **1**-Solv complexes (Table 3) are in good agreement with the experimental activation enthalpies, providing further support for the dissociative mechanistic assignment. The calculated BDE for the **1**-(η^1-O–DHF) bond is ≈4 kcal/mol lower than that of **1**-THF consistent with the reduced donor ability of the oxygen due to delocalization of its lone pairs within the π system of the DHF ligand.

An enthalpic profile for the isomerization reaction **1**-(η^1-O–DHF) → **1**-(η^2-DHF) was obtained and is shown in Figure 10. Consistent with the experimental observation, the η^2 bound adduct is calculated to be the thermodynamic product while the oxo isomer is found to be only 1.6 kcal/mol higher in energy. This small difference in binding enthalpy is similar to the ≈2 kcal/mol difference in the estimated BDEs for the analogous **1**-THF and **1**-(η^2-cyclohexene) complexes. The calculated $\Delta H^{\ddagger}$ = 10.7 kcal/mol for the isomerization reaction is in excellent agreement with the experimental value of 11.2 ± 0.3 kcal/mol. Consistent with the experimental findings, the calculations suggest that the metal migrates from one functional group to another forming a transition state with the Fe atom almost equidistant from the oxygen and one edge of the olefinic bond (Figure 11). The Fe–O bond length increases from 2.120 Å in **1**-(η^1-O–DHF) to 3.046 Å in the transition state. The Fe–C1 and Fe–C2 bond lengths increase from 2.432 and 2.304 Å in **1**-(η^2- DHF) to 3.151 and 3.739 Å in the transition state, respectively. Any developing interaction between the Fe atom and the olefinic bond in the transition state is not reflected in the C=C bond length as the 1.323 Å distance is the same as that in free DHF (1.324 Å).

CONCLUDING REMARKS

In summary, photolysis of the [FeFe]-hydrogenase model compound, (μ-pdt)[Fe(CO)$_3$]$_2$ (**1-CO**), in cyclohexane solution in the presence of weakly binding solvents (Solv = cyclohexene, 3-hexyne, 2,3-DHF, and THF) results in CO loss with formation of transient (μ-pdt)[Fe(CO)$_3$][Fe(CO)$_2$(Solv)] (**1**-Solv) complexes. Displacement reactions of the solvate in **1**-Solv with the stronger binding ligands, *cis*-cyclooctene and pyridine, were shown to occur via a dissociative mechanism. Temperature dependent kinetic data have provided reliable estimates of the **1**-Solv bond dissociation energies which were found to be in very good agreement with calculated values obtained from DFT studies. Upon photolyzing **1**-CO in the presence of the ambidentate ligand, 2,3-dihydrofuran, where olefin or oxygen binding is possible, an O-bonded kinetic product was first observed followed by intramolecular rearrangement to the thermodynamically more stable olefin bound complex.

It is not likely that light-induced ligand dissociation/ligand exchange is a property of the [FeFe]-hydrogenase active site, except in degradation reactions. However, it is clear that diiron molecules such as (μ-pdt)[Fe(CO)$_3$]$_2$ that serve as precursors to more faithful models of the 2-Fe subsite of the H-cluster have unique properties. As demonstrated above, these chemical/reactivity properties may be creatively exploited. The range of CO/L substituted diiron compounds in (μ-pdt)[Fe(CO)$_2$L]$_2$ or (μ-pdt)[Fe(CO)$_2$L]{Fe(CO)$_2$L′] possibly exceeds any known dinuclear scaffold in inorganic/organometallic chemistry. The study of the photochemical release of CO and subsequent clean formation of products with thermally labile ligands add to a repertory of possible selective synthetic routes to sophisticated constructs with designed CO/L substitution patterns. In this way, catalytic features beyond hydrogen processing might be envisaged for such base metal compounds as are intimated in nature's synthetic toolbox.

ASSOCIATED CONTENT

Supporting Information

Additional figures, including difference IR spectra for several **1**-Solv and **1**-L complexes, and a plot of k_{obs} vs [pyridine] for the displacement of DHF from **1**-(η^2-DHF). This material is available free of charge via the Internet at http://pubs.acs.org.

AUTHOR INFORMATION

Corresponding Author

*E-mail: djdarens@mail.chem.tamu.edu (D.J.D.).

Notes

The authors declare no competing financial interest.

ACKNOWLEDGMENTS

This publication was made possible by funding from the Qatar National Research Fund (a member of Qatar Foundation). The experimental work was supported by NPRP grant no. 09-157-1–024 and the theoretical studies by NPRP grant no. 09-143-1–022. Synthetic studies of the iron carbonyl derivatives were supported by NSF grants (CHE-0910679 and CHE-1057743). The statements made herein are solely the responsibility of the authors.

REFERENCES

(1) *Hydrogen as a Fuel, Learning from Nature*; Cammak, R., Frey, M., Robson, R., Eds.; Taylor & Francis, Inc.: New York, 2001.

(2) (a) Felton, G. A. N.; Mebi, C. A.; Petro, B. J.; Vannucci, A. K.; Evans, D. H.; Glass, R. S.; Lichtenberger, D. L. *J. Organomet. Chem.* **2009**, *694*, 2681–2699. (b) Capon, J.-F.; Gloaguen, F.; Pétillon, F. Y.; Schollhammer, P.; Talarmin, J. *Coord. Chem. Rev.* **2009**, *253*, 1476–1494.

(3) Liu, T.; Darensbourg, M. Y. *J. Am. Chem. Soc.* **2007**, *129*, 7008–7009.

(4) Li, H.; Rauchfuss, T. B. *J. Am. Chem. Soc.* **2002**, *124*, 726–727.

(5) Singleton, M. L.; Bhuvanesh, N.; Reibenspies, J. H.; Darensbourg, M. Y. *Angew. Chem., Int. Ed.* **2008**, *47*, 9492–9495.

(6) Ridley, A. R.; Stewart, A. I.; Adamczyk, K.; Ghosh, H. N.; Kerkeni, B.; Guo, Z. X.; Nibbering, E. T. J.; Pickett, C. J.; Hunt, N. T *Inorg. Chem.* **2008**, *47*, 7453−7455.
(7) Kania, R.; Frederix, P. W. J. M.; Wright, J. A.; Ulijn, R. V.; Pickett, C. J.; Hunt, N. T. *J. Chem. Phys.* **2012**, *136*, 044521.
(8) Marhanke, J.; Pierri, A. E.; Lomotan, M.; Damon, P. L.; Ford, P. C.; Works, C. *Inorg. Chem.* **2011**, *50*, 11850−11852.
(9) Brown-McDonald, J.; Berg, S.; Peralto, M.; Works, C. *Inorg. Chim. Acta* **2009**, *362*, 318.
(10) Kaziannis, S.; Santabarbara, S.; Wright, J. A.; Greetham, G. M.; Towrie, M.; Parker, A. W.; Pickett, C. J.; Hunt, N. T. *J. Phys. Chem. B* **2010**, *114*, 15370.
(11) Silaghi-Dumitrescu, I.; Bitterwolf, T. E.; King, R. B. *J. Am. Chem. Soc.* **2006**, *128*, 5342.
(12) Zhao, X.; Georgakaki, I. P.; Miller, M. L.; Yarbrough, J. C.; Darensbourg, M. Y. *J. Am. Chem. Soc.* **2001**, *123*, 9710.
(13) Frisch, M. J.; et al.*Gaussian Development Version, Revision H.08*; Gaussian, Inc.: Wallingford CT, 2009.
(14) Chai, J.-D.; Head-Gordon, M. *Phys. Chem. Chem. Phys.* **2008**, *10*, 6615.
(15) Weigend, F.; Ahlrichs, R. *Phys. Chem. Chem. Phys.* **2005**, *7*, 3297.
(16) Zhang, Y.; Hu, M.-Q.; Wen, H.-M.; Si, Y.-T.; Ma, C.-B.; Chen, C.-N.; Liu, Q.-T. *J. Organomet. Chem.* **2009**, *694*, 2576.
(17) Schultz, R. H. *Int. J. Chem. Kinet.* **2004**, *36*, 427.
(18) Zheng, Y.; Wang, W.; Lin, J.; She, Y.; Fu, K.-J. *J. Phys. Chem.* **1992**, *96*, 7650.
(19) Coleman, J. E.; Dulaney, K. E.; Bengali, A. A. *J. Organomet. Chem.* **1999**, *572*, 65.
(20) Angelici, R. J.; Loewen, W. *Inorg. Chem.* **1967**, *6*, 682.
(21) While cyclohexane has a melting point of only ≈280 K, in the presence of 6.6 M DHF, the solution remained unfrozen until ≈203 K.
(22) Bengali, A. A.; Hall, M. B.; Wu, H. *Organometallics* **2008**, *27*, 5826.